

LINC01224 promotes gastric cancer development via miR-193a-5p/YES1 pathway

Yansong Pu^{1,*}, Yi Liu^{2,*}, Fei Xue¹, Qingguo Du¹, Yu Ma³, Baojun Duan², Min Wu⁴, Yanbin Long¹, Jianhua Wang¹

¹The Second Department of General Surgery, Shaanxi Provincial People's Hospital, Beilin, Xi'an 710068, P.R. China

²Department of Medical Oncology, Shaanxi Provincial People's Hospital, Beilin, Xi'an 710068, P.R. China

³Department of Pathology, Shaanxi Provincial People's Hospital, Beilin, Xi'an 710068, P.R. China

⁴Office of Scientific Research, Shaanxi Provincial People's Hospital, Beilin, Xi'an 710068, P.R. China

*Equal contribution

Correspondence to: Jianhua Wang; email: wangjianhuaman@163.com, <https://orcid.org/0000-0002-5276-5078>

Keywords: long non-coding RNA, gastric carcinoma, LINC01224, miR-193a-5p, YES1

Received: December 27, 2020 **Accepted:** September 18, 2021 **Published:**

Copyright: © 2021 Pu et al. This is an open access article distributed under the terms of the [Creative Commons Attribution License](https://creativecommons.org/licenses/by/3.0/) (CC BY 3.0), which permits unrestricted use, distribution, and reproduction in any medium, provided the original author and source are credited.

ABSTRACT

Gastric cancer (GC) is one of the most common malignant tumors of the digestive tract with a high degree of malignancy. There is considerable evidence that long non-coding RNA (lncRNA) is associated with the progression of GC. However, the relationship between LINC01224 and GC has not yet been elucidated. Here, we found that LINC01224 was highly expressed in GC and correlated with shortened overall survival time by bioinformatics analysis. We further confirmed that LINC01224 was highly expressed in GC specimens, which was positively correlated with TNM staging and shortened overall survival time. The bioinformatics analysis revealed that LINC01224 might be involved in regulating the proliferation and cell cycle of GC cells. Functional experiments further confirmed that knockdown of LINC01224 inhibited the proliferation of GC cells and induced apoptosis and G1 phase cell cycle arrest of GC cells. Besides, silencing of LINC01224 inhibited the growth of GC cells *in vivo*. Mechanistically, LINC01224 promoted the expression level of YES1 in GC cells by competitively binding to miR-193a-5p. Additionally, miR-193a-5p inhibitor and up-regulation of YES1 reversed the effects of knockdown of LINC01224 on the proliferation, apoptosis, and cell cycle of GC cells, whereas transfected mutant-LINC01224 plasmids did not. Our findings confirmed that LINC01224 could be a potential prognostic marker for GC. The LINC01224/miR-193a-5p/YES1 axis plays a vital role in the proliferation, cell cycle, and apoptosis of GC cells, and it could be a potentially important diagnostic and therapeutic target for GC.

INTRODUCTION

Gastric cancer (GC) is a prevalent digestive tract malignancy. According to cancer statistics published in 2018 [1], the incidence of GC was 5.7% of all types of cancer diagnosed worldwide, ranking sixth, with GC-related deaths accounting for about 8.2% of all cancer-related deaths, ranking second [2]. GC cells are highly malignant and grow fast, leading to a rapid

progression and easy metastasis of GC. Targeted therapy for GC has markedly attracted clinicians' attention in recent years, while its efficacy is still unsatisfactory. Therefore, it is critical to study mechanisms driving GC development and to establish novel therapeutic targets for treating GC.

A great number of genetic and molecular changes, including oncogene activation, tumor suppressor gene

inactivation, microsatellite instability and epigenetics, have been proved participate in GC initiation. Long non-coding RNAs (lncRNAs) are a type of RNAs whose transcript lengths exceed 200 nucleotides. They were initially considered as the "noise" of genome transcription and had no biological role [3]. Nonetheless, recent investigations illustrated that lncRNAs regulate the biological functions of cells through a variety of pathways and mechanisms, and are associated with the pathogenesis of tumors and other diseases [4]. LINC01224, as a newly discovered lncRNA participates in the malignancy of liver cancer [5] and ovarian cancer [6]. However, the relationship between LINC01224 and GC has still remained elusive. We previously established that LINC01224 was expressed highly in GC tissues by the assessment of data collected from the Genotype-Tissue Expression (GTEx) data resources as well The Cancer Genome Atlas (TCGA), however, its role and mechanism in malignant progression of GC require further research.

Research evidence opines that lncRNAs have an indispensable role in chromatin modification, genomic imprinting, post-transcriptional modulation, transcriptional activation, protein function regulation, and other related signal transduction and regulation processes [7]. Recently, a new model of lncRNAs being involved in gene regulation, namely competitive endogenous RNA (ceRNA), has been suggested [8]. This model opines that if lncRNAs and mRNAs have same miRNA binding regions (MREs), which can be recognized by same miRNAs, they can competitively bind to the common miRNAs and influence each other's expression. These interactions among mRNA, miRNA and lncRNA create complex regulatory networks. lncRNAs work as sponges of miRNAs, influencing the expression levels of protein-encoding genes, hence promoting the onset and progress of tumors [9]. As targets of lncRNAs, miRNAs contribute to malignant behaviors. It is noteworthy that miRNAs play indispensable biological roles in promoting or inhibiting tumorigenesis through interacting with cancer-related proteins. Reduced miR-193a-5p level in cancer cells has been documented [10], and it could play a role as a cancer repressor [11]. LINC01234 modulates the level of CCNE1 expression docking to miR-193a-5p, influencing the development of esophageal cancer [12]. Nonetheless, the relationship of LINC01224 with miR-193a-5p, as well as the role of LINC01224 in GC have still remained elusive.

Herein, we explored the expression level, as well as the function of LINC01224 in GC. We established that LINC01224 showed high expression in GC cell lines

and tissues. Down-regulation of LINC01224 dampened GC cell growth, enhanced the cell apoptosis and G1 phase arrest, and inhibited *in vivo* tumor growth. Besides, we found that LINC01224 regulated the expression level of YES proto-oncogene 1 (*YES1*) by competitive adsorption of miR-193a-5p. Overexpression of wild-type-LINC01224 (wt-LINC01224), rather than mutant-LINC01224 (mut-LINC01224) containing mutations at the putative miR-193a-5p binding site, could revert the repressive function of miR-193a-5p.

MATERIALS AND METHODS

Ethical statement

The Ethics Committee of Shaanxi Provincial People's Hospital (Shaanxi, China) granted approval of this research work. All subjects signed the written informed consent form before enrollment. All animal experiments were carried out as per policies of the National Institutes of Health (NIH) Guide for the Care and Use of Laboratory Animals.

Bioinformatics analysis

The differential expression of LINC01224 in GC along with non-malignant tissues was analyzed by the GEPIA using the data collected from TCGA and GTEx data resources [13]. The RNA-seq transcriptome profiling data and clinical files related to GC patients and healthy controls in TCGA and GTEx databases were downloaded from the Xena (<https://xenabrowser.net/datapages/>). The InCAR website (<https://lncar.renlab.org/>) was adopted to analyze the association of the expression level of LINC01224 with overall survival (OS) in the GSE38749 dataset for individuals with GC. The differential analysis of transcriptome data was carried out using R's edgeR package, with the screening cut-off of $|\log_2 \text{fold-change (FC)}| > 2.0$ along with a $P < 0.05$. Limma package was adopted to perform the correlation analysis, and the screening threshold and the correlation coefficient were $P < 0.001$ and $R > 0.50$, respectively. The possible biological functions and pathways of LINC01224 in GC samples were analyzed by the GO along with KEGG pathway enrichment analyses using the co-expressed genes. The "enrichplot" package was used for the GO along with KEGG analyses. Based on the level of LINC01224, GC patients were stratified into low expression group ($n = 188$) and high expression group ($n = 187$), and the effects of the expression level of LINC01224 on various biological pathways were analyzed by the GSEA (gene set enrichment analysis) [14]. The GSEA obtained genes served as the reference gene sets, with

each analysis repeated 1000 times, as per the default weighted enrichment statistical approach [15].

Clinical data collection

We collected 294 GC and paired distal paracancerous tissue samples from patients with GC (male (162) versus female (132); mean age, 60.4 ±10.7 years old) who underwent surgery in Shaanxi Provincial People's Hospital from January 1, 2015 to December 31, 2017. No patients received chemoradiotherapy before pathological confirmation of the diagnosis of GC. Overall, 48 cases were of highly differentiated adenocarcinoma, 149 cases of moderately differentiated adenocarcinoma, 76 cases of poorly differentiated adenocarcinoma, and 21 cases of undifferentiated adenocarcinoma. GC staging was on the basis of the American Joint Committee on Cancer (AJCC) Tumor, Node, Metastasis (TNM) staging system. GC tissues and paired distal paracancerous tissues (more than 5 cm away from GC tissues) were collected during the surgery and cryopreserved in liquid nitrogen or immersed in neutral formaldehyde.

Immunohistochemistry (IHC)

Cancer tissue, paracancerous tissue, and xenograft tissue were fixed with formalin, paraffin-embedded, and chopped into segments with a thickness of 5 µm. After dewaxing, dehydration, and antigen blocking, tissue sections were inoculated overnight with anti-YES1 antibody (Cat No. ab109265, Abcam, UK, 1:100) or anti-Ki-67 antibody (Cat No. BM4381, Boster, China, dilution, 1:100) at 4° C. Then, IHC was performed using the two-step immunohistochemical kit (Cat No. SV0002, Boster, China) as described in the manual of the manufacturer.

RT-qPCR

Total RNA was purified from tissues, as well as cells using the TRIzol reagent (Cat No. 15596026, Invitrogen, USA). The PrimeScript™ 1st Strand cDNA Synthesis kit (Cat No. 6210B, Takara, Japan) was utilized to reversely transcribe total RNA into cDNA. Besides, the TB Green Premix Ex Taq II kit (Cat No. RR820Q, Takara, Japan) was employed to assay the mRNA and transcript levels of lncRNAs on the ABI7500 system (Applied Biosystems Inc., USA). *GAPDH* served as the standard. The microRNA was detected with the Mir-X miRNA qRT-PCR TB Green Kit (Cat No. 638314, Takara, Japan). We repeated each experiment at least 3 times, and the $2^{-\Delta\Delta CT}$ approach was applied for determination of gene expression. Oligonucleotides used for RT-qPCR are given in Supplementary Table 1.

Cell culture

The GC cell lines (HGC-27, KATO III, SNU-1, AGS, and NCI-N87) and the non-malignant human gastric epithelial GES-1 cell line were supplied by Procell Life Science and Technology Co., Ltd. (China). HGC-27, SNU-1, as well as NCI-N87 cells were inoculated in RPMI-1640 medium enriched with 10% FBS. Besides, the KATO III cells were inoculated in the IMDM enriched with 10% FBS, and AGS and AGS-Luc2 cells were cultured in the Ham's F-12 medium enriched with 10% FBS. According to the conditions of the cell growth, the culture medium was replaced every 3 days. When the cell fusion level reached 80-90%, the cells were accordingly passaged.

Transfection

Short hairpin RNAs of LINC01224 (sh-LINC01224-1 and sh-LINC01224-2) and *YES1* (sh-YES1) were designed and synthesized to knock down the expression level of LINC01224 and *YES1*, and shRNA-control was set as a negative control (NC). The sequences of shRNA are shown in Supplementary Table 1. To establish a cell line stably lacking LINC01224 expression, the shRNA-1 of LINC01224 was cloned into the pLKO.1 plasmid. The recombinant plasmids, along with packaging, as well as envelope plasmids (psPAX2 and pMD2.G), were co-transferred into HEK 293T cells for lentiviral packaging. Post 48 h of transfection, lentiviral particles were collected to infect AGS cells with polybrene. Puromycin was used to screen the stably transfected cell lines. To up-regulate the expression levels of LINC01224 and *YES1*, cDNAs of LINC01224 and *YES1* were synthesized via PCR, then subcloned into the pcDNA3.1 plasmid separately. The starBase [16] was employed to predict the prospective docking sites of miR-193a-5p on LINC01224 and *YES1*. The potential docking sites of miR-193a-5p on LINC01224 were mutated using the site-directed mutation kit (Cat No. SDM-15, Sbsgene, China) to synthesize mutant-LINC01224. The pcDNA3.1 empty vector was set as an NC. The mimics of miR-4436a, miR-2467-3p, miR-193a-5p, miR-650, miR-3612, miR-5000-3p, miR-6884-5p, miR-29b-3p, miR-29a-3p, miR-29c-3p, and inhibitors of miR-193a-5p were designed and synthesized by GenePharma (China).

Dual-luciferase reporter assay

We cloned the full-length sequences of LINC01224 cDNA and *YES1* 3'-UTR and then them inserted into the pmirGLO Dual-Luciferase enzyme Vector (Cat No. e1330, Promega, USA), which were named pmirGlo-LINC01224-wt and pmirGlo-YES1-wt, respectively. Then, pmirGlo-LINC01224-mut and

pmirGlo-YES1-mut plasmids were synthesized by RiboBio Co., Ltd. (China). The pRL-TK plasmid (Cat No. e2241, Promega) was used as a control. After that, miRNA mimics and miRNA mimic controls were co-propagated into AGS cells with the luciferase enzyme reporter plasmid using the Lipofectamine 2000. Post 48 h of transfection, the luciferase enzyme activity was detected by the Dual-Luciferase enzyme Reporter Gene Assay kit (Cat No. RG027, Beyotime, China).

RNA pull-down assay

The Pierce RNA 3'End Desthiobio-tinylation kit (Cat No. 20163, Thermo, USA) was used to label miR-193a-5p (Bio-miR-193a-5p). It was incubated with Streptavidin-agarose beads (Cat No. 16-126, Millipore, USA) at 4° C for 1 h, and then, incubated with lysed cells. After washing the magnetic beads, the bound RNA was isolated using the TRIzol reagent, and RNA isolated from the cell lysates was used as a control for the total input. The RT-qPCR was then performed to analyze the cross talk of LINC01224 with miR-193a-5p.

RNA immunoprecipitation (RIP) assay

It was established that the relationship of miRISC (miRNA-bound RNA-induced silencing complex) with target mRNAs could result in deadenylation-mediated target mRNA decapping along with degradation. To indicate whether miR-193a-5p can modulate the expression level of LINC01224 through RISC, RIP analysis was undertaken on AGS cells using AGO2 antibodies. Cells in each group were lysed with the RIP lysis buffer, and the cell lysates were inoculated with magnetic beads coated with AGO2 antibody or NC immunoglobulin G (IgG) antibody. RNA was purified and analyzed by the RT-qPCR.

CCK-8 assay

AGS and SNU-1 cells were inoculated into a 96-well plate with the density of 2000 cells/well. After 24 h of culture, 10 µL of CCK-8 reagent (Cat No. C0038, Beyotime, China) was added into each well and allowed to incubate for 2 h, and the absorbance at wavelength of 450 nm was determined with a microplate reader.

Colony formation assay

AGS and SNU-1 cells were inoculated into 6-well plates (500 cells/well), and after two weeks of culture, they were fixed with 4% PFA, stained with 1 mL of crystal violet staining solution for 5 minutes, then counted under a microscope.

EdU assay

4×10³ cells/well were planted into a 96-well plate. Each well was incubated with a medium containing 100 µL of 50 µM EdU for two hours. The cells were fixed, permeated, and stained as described by the manufacturer (Cat No. C10310-1/-2/-3, RiboBio, China). The nucleus was stained (in 1 mg/mL DAPI) for 20 minutes.

Flow cytometry

We collected the cells from each group, and cell cycle changes were detected by flow cytometry after PI staining; the rate of cell apoptosis was explored via flow cytometry after Annexin V-FITC/PI double staining (Cat No. C1062S, Beyotime, China).

Western blot assay

Protein samples were extracted, purified and then quantitated, followed by fractionation on SDS-PAGE gels. Afterward, they were blotted onto PVDF membranes, which were then inoculated overnight with YES1 (Cat No. ab109265, Abcam, 1:3000), AGO2 (Cat No. ab32381, Abcam, 1:1000), and GAPDH (Cat No. ab181602, Abcam, 1:10000) antibodies diluted with 5% skim milk at 4° C. The membranes were probed for 30 minutes with HRP-labelled secondary antibodies (Cat No. BA1051 or BA1055, Boster, 1:2000) diluted with 5% skim milk at room temperature, and the binding was assessed by the Immobilon Western HRP Substrate (Cat No. WBKLS0100, Millipore, USA) on the ChemiDoc MP system (Bio-Rad, USA). Images of protein bands were acquired, and Image Software was adopted to analyze the gray value. GAPDH served as the normalization standard.

A nude mouse xenograft model and *in vivo* imaging

We raised six-week-old male BALB/c nude mice were divided into 3 groups: sh-control, sh-LINC01224-1, and sh-LINC01224-2 (n = 6 mice in each group). After general anesthesia, a transfected AGS-Luc2 cell suspension (1×10⁶ cells/200 µL) was seeded into the right armpit of nude mice. All mice were fed in the same controlled environment and were evaluated every 3 days. The length along with width of the tumor was documented in detail. Tumor volume was computed using the following formula: Tumor volume = (length × width²)/2. After 16 days, D-luciferin potassium salt (Cat No. ab143655, Abcam) was injected intraperitoneally, and the XENOGEN IVIS system was used for *in vivo* imaging. We euthanized the nude mice, imaged the tumors, and weighed them.

Statistical analyses

All data analyses were implemented in SPSS 21.0 software (IBM, USA). Counting data are given as numbers or percentages and analyzed by the χ^2 test. Values are presented as mean \pm standard deviation. The Students' t-test was used to compare the measured data between two groups. Data across multiple groups were compared using one-way analysis of variance (ANOVA). The data of different time points were compared by the repeated measures ANOVA. $P < 0.05$ signified statistical significance.

Data sharing statement

The datasets used and/or analyzed during the current study are available from the corresponding author on reasonable request.

Ethical statement

The study was conducted with the approval of the ethics committee of Shaanxi provincial people's hospital. All patients in the study signed written informed consent before enrollment. All animal experiments were conducted under the international commission's guidelines for the care and use of laboratory animals.

RESULTS

LINC01224 expression is enriched in GC

We performed analysis of TCGA along with GTEx data resources using the GEPIA, and found that GC tissues have higher levels of LINC01224 than non-malignant tissues (Figure 1A). We also analyzed the expression of LINC01224 in TCGA database alone, and the data

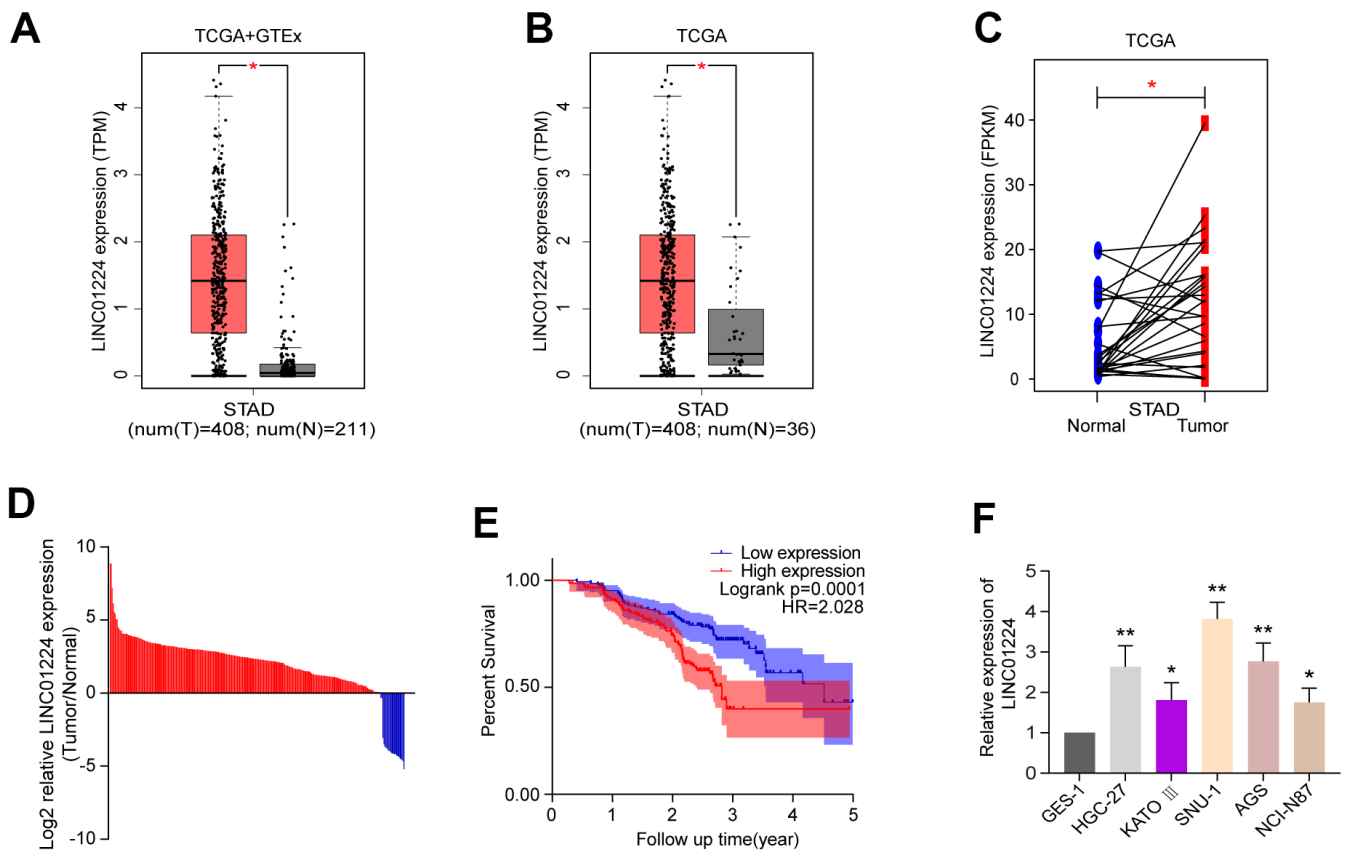


Figure 1. The expression of LINC01224 is up-regulated in gastric cancer tissues and cells and is related to the prognosis of patients with gastric cancer. (A) Comparison of LINC01224 expression in gastric cancer tissues (red) and normal tissues (grey) from TCGA-STAD datasets and GTEx datasets. (B) Expression of LINC01224 in gastric cancer tissues (red) and adjacent tissues (grey) from TCGA Dataset. (C) Expression of LINC01224 in 27 pairs of gastric cancer tissues (red) and corresponding paracancerous tissues (blue) from TCGA datasets. (D) Expression of LINC01224 in 294 pairs of gastric cancer tissues and corresponding paracancerous tissues was detected by qRT-PCR. (E) Our cohort of gastric cancer patients was analyzed for postoperative survival based on LINC01224 expression by Kaplan-Meier survival analysis. (F) Expression of LINC01224 in gastric cancer cell lines (HGC-27, KATO III, SNU-1, AGS and NCI-N87) and normal gastric mucosal epithelial cell lines (GES-1) was detected by qRT-PCR.

illustrated that in comparison with non-malignant tissues, LINC01224 was elevated in cancerous tissues (Figure 1B). Further analysis uncovered differential LINC01224 expression between 27 matched GC tissues and vicinal non-malignant tissues (Figure 1C). GC and neighboring non-malignant tissues were collected from 294 GC patients. The RT-qPCR data illustrated that in comparison with neighboring non-malignant tissues, the expression level of LINC01224 was remarkably higher in GC tissues, which is congruent with the data of bioinformatics analysis (Figure 1D). We further evaluated the relationships of the expression level of LINC01224 with the clinicopathological characteristics of individuals with GC. GC patients were stratified into a high expression group ($n = 147$) and a low expression group ($n = 147$), per the median expression level of LINC01224. Table 1 summarizes patients' demographic and clinical characteristics and their associations with LINC01224 level. The expression level of LINC01224 was remarkably linked to the depth of tumor infiltration ($P = 0.041$) and TNM stage ($P < 0.001$). There was no remarkable relationship of LINC01224 and patients' clinical data at baseline, such as gender and age ($P > 0.05$). The Kaplan-Meier data illustrated that the post-operative survival of individuals with GC harboring high LINC01224 levels was markedly lower in contrast with those individuals with GC in the low levels of LINC01224 ($P = 0.0001$, hazard ratio (HR) = 2.028, Figure 1E). Analysis of TCGA database by using the GEPIA uncovered that OS rate of individuals with GC with high LINC01224 levels was lower contrasted with that of individuals with GC in the low expression group ($P = 0.086$, HR = 1.4, Supplementary Figure 1A). The analysis performed using the InCAR website indicated that individuals with GC exhibiting high expression had a lower OS rate contrasted with those in the low expression group ($P = 0.0342$, HR = 5.4281, Supplementary Figure 1B). Besides, the data of the univariate along with multivariate survival assessments further clarified the relationship of the level of LINC01224 with GC prognosis. As illustrated in Table 2, the univariate survival data identified two prognostic factors: the expression level of LINC01224 ($P < .001$), as well as the TNM stage ($P < 0.001$). Meanwhile, the multivariate survival data illustrated that TNM stage and LINC01224 were independent prognostic biomarkers for GC. Moreover, we found that the expression of LINC01224 in GC cell lines (HGC-27, KATO III, SNU-1, AGS, and NCI-N87) were higher contrasted with that in the GES-1 cells ($P < 0.05$, Figure 1F).

Prediction of the molecular function of LINC01224

To explore how LINC01224 affects GC cell lines, we analyzed the genes co-expressed with LINC01224 using

TCGA and GTEx databases (Figure 2A). Then, the GO along with KEGG assessments were performed based on the genes co-expressed with LINC01224 (Figure 2B, 2C). The GO enrichment analysis revealed that the genes co-expressed with LINC01224 were associated with the organelle fission, chromosome segregation, DNA replication, as well as nuclear division (Figure 2B). The KEGG data illustrated that the expression level of LINC01224 was correlated to signal transduction cascades, consisting of cell cycle, cellular senescence, GC, and DNA replication (Figure 2C). The GSEA data illustrated that the expression level of LINC01224 was linked to the cell cycle, p53 signaling cascade, DNA replication, modulation of autophagy, mismatch repair, along with nucleotide excision repair. On the basis of the bioinformatics analyses, we hypothesized that LINC01224 could participate in regulating the growth along with the cell cycle of GC cells.

Knockdown of LINC01224 markedly repressed the cell growth and triggered the apoptosis of GC cells

To verify the data of the bioinformatics analyses, we silenced LINC01224 expression in GC cells by sh-RNA and detected changes in the cell cycle, proliferation, and apoptosis. We established that LINC01224 was elevated in the GC cell lines (SNU-1 and AGS). Thus, we selected these two cell lines to knock down LINC01224 (Figure 3A). The CCK-8 data illustrated that the silencing of LINC01224 could remarkably inhibit the proliferation of SNU-1, as well as AGS cells (Figure 3B). The colony formation along with EdU assays data illustrated that dampening of LINC01224 could noticeably repress the growth of SNU-1 and AGS cell lines (Figure 3C, 3D). The results of Annexin V-PI staining-flow cytometry suggested that the apoptosis rate of GC cells was remarkably elevated after silencing of LINC01224 (Figure 3E). The knockdown of LINC01224 caused the blockage of SNU-1, as well as AGS cells in the G1 phase (Figure 3F).

Silencing of LINC01224 dampened the growth of GC cells *in vivo*

To clarify the relationship of LINC01224 with the growth of GC cells *in vivo*, AGS cells with LINC01224 knockdown were inoculated subcutaneously into nude mice. It was found that knockdown of LINC01224 remarkably dampened the tumor growth in mice ($P < 0.05$, Figure 4A), as revealed by the tumor growth curve ($P < 0.05$, Figure 4B) and tumor weight ($P < 0.05$, Figure 4B). The Ki-67 staining illustrated that there were fewer Ki-67-positive cells in LINC01224-knockdown group than in controls ($P < 0.05$, Figure 4C). The data of RT-qPCR illustrated that the

Table 1. Correlation between the clinicpathologic characteristics and LINC01224 expression in 294 GC patients.

Characteristics	n=294	LINC01224		P
		Low expression(n=147)	High expression(n=147)	
Age(y)				0.171
	<60	115	59	
	≥60	179	88	
Gender				0.482
	Male	162	78	
	Female	132	69	
Tumor invasion depth				0.041
	T1-2	111	64	
	T3-4	183	83	
Lymph node metastasis				0.073
	Negative	86	50	
	Positive	208	97	
Distant metastasis				0.304
	M0	278	141	
	M1	16	6	
TNM stage				<0.001
	I+II	150	91	
	III+IV	144	56	

Table 2. Univariate and multivariate analysis of the correlation of clinic pathological parameters with OS in 294 GC patients.

Parameter	Univariate analysis		Multivariate analysis	
	HR(95%CI)	P-value	HR(95%CI)	P-value
Gender	1.12(0.77-1.63)	0.55		
Age	1.00(0.99-1.02)	0.57		
TNM stage	4.28(3.25-5.64)	<0.001	3.62(2.66-4.91)	<0.001
LINC01224 expression	1.70(1.44-2.00)	<0.001	1.24(1.05-1.47)	0.01

expression of LINC01224 in the LINC01224-knockdown group was lower in comparison with that in the controls ($P < 0.05$, Figure 4C). We found that sh-LINC01224-1 had a better knockdown effect. Thus, it was adopted for subsequent experiments. Collectively, the above-mentioned results demonstrated that silencing of LINC01224 repressed the GC cell growth *in vivo*.

LINC01224 exhibited to works as a molecular sponge for miR-193a-5p in GC cells

We used two online platforms (CPAT and CPC) to predict the protein-coding ability of LINC01224, and the result was consistent with that reported previously [5], which showed that LINC01224 has no protein-coding ability (Supplementary Figure 2). We further

determined the subcellular localization of LINC01224 in SNU-1, as well as AGS cells by *in situ* hybridization (Figure 5A) and nuclear-cytoplasmic fractionation (Figure 5B), and found that LINC01224 was primarily expressed in the cytoplasm. Research evidence illustrates that LINC01224 acts as a "sponge" of miRNAs in ovarian cancer [17] and hepatocellular carcinoma [5]. We attempted to investigate whether LINC01224 has a similar ceRNA effect in GC cells. For this purpose, we used the starBase and DIANA-LncBase to predict the potential miRNA targets of LINC01224 (Figure 5C). It was found that a total of 10 miRNAs (miR-4436a, miR-2467-3p, miR-193a-5p, miR-650, miR-3612, miR-5000-3p, miR-6884-5p, miR-29b-3p, miR-29a-3p, and miR-29c-3p) could bind to LINC01224. Then, the relationships between the

candidate miRNAs and LINC01224 in AGS cells were tested by the dual-luciferase enzyme reporter assay. It was established that the luciferase enzyme activity decreased when miR-193a-5p mimics were added (Figure 5D). Therefore, miR-193a-5p was adopted in the follow-up tests. The data of the dual-luciferase enzyme reporter assay illustrated that miR-193a-5p mimics decreased the luciferase enzyme activity of reporter plasmids containing wt-LINC01224, rather than mut-LINC01224 (Figure 5E). It is noteworthy that the expression of LINC01224 was down-regulated after overexpression of miR-193a-5p in AGS cells (Figure 5F). The data of the RNA pull-down experiment suggested that LINC01224 could be pulled down by biotin-labeled miR-193a-5p (Figure 5G). AGO2 is the

key component of RISCs, which guides RISCs to silence target mRNAs by shearing them, transcriptional repression, or deadenylation [18]. We found that LINC01224 and miR-193a-5p were remarkably enriched in the AGO2-containing protein complexes by the RIP assay (Figure 5H). These findings exhibited that miR-193a-5p could dock to LINC01224 and cause its degradation in GC cells.

LINC01224 acted as a ceRNA in GC cells to promote the expression level of *YES1* by adsorbing miR-193a-5p

We used the online websites (miRDB, miRDIIP, and miRWalk) to forecast the target genes of miR-193a-5p.

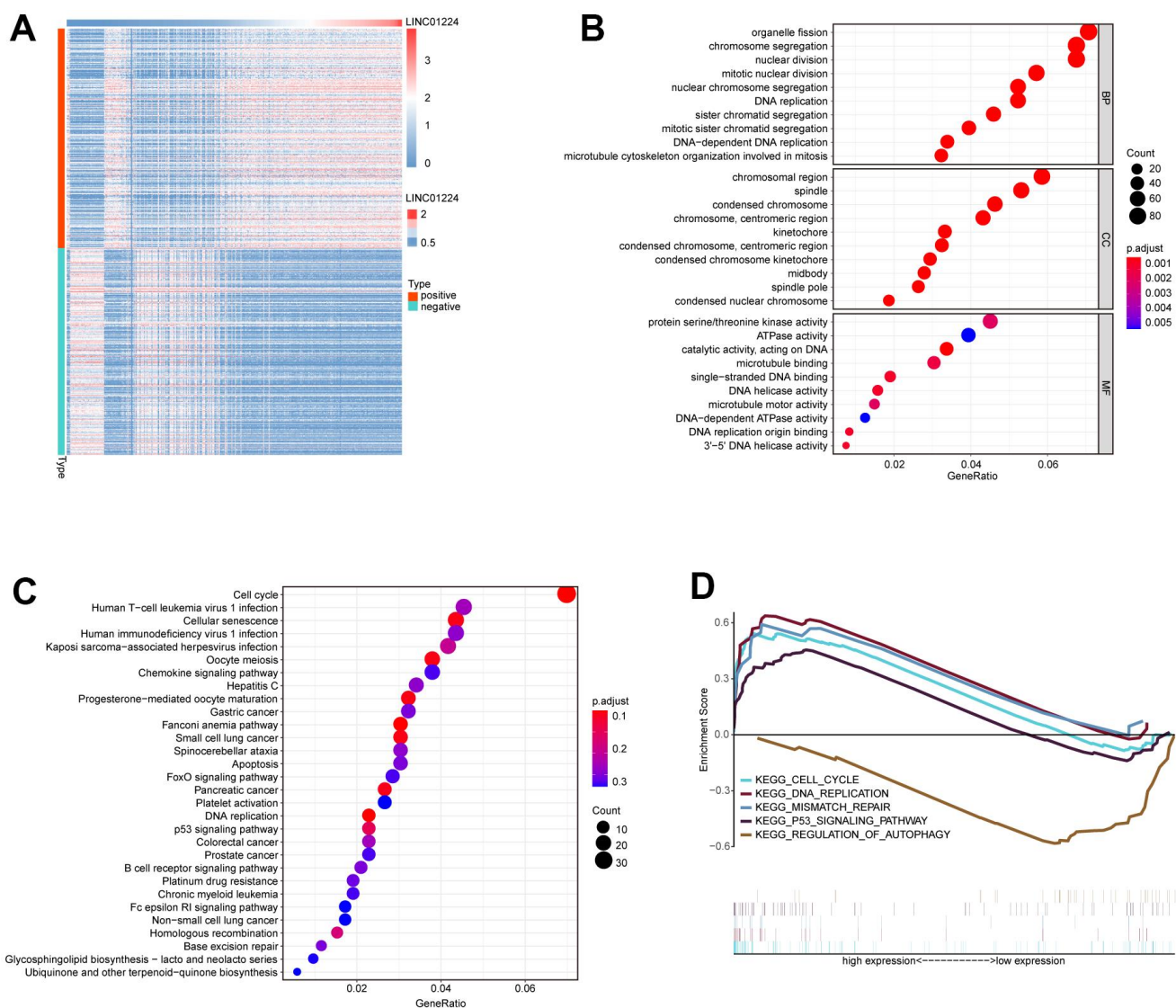


Figure 2. Bioinformatics predicts the biological functions of LINC01224. (A) Heat map of protein-coding genes with co-expression relationship with LINC01224. (B) GO functional annotation based on protein-coding genes co-expressed with LINC01224. (C) KEGG pathway enrichment analysis based on protein-coding genes co-expressed with LINC01224. (D) GESA analysis based on LINC01224 expression.

Among them, genes positively correlated to the expression level of LINC01224 were selected: *KDELR3*, *XYLB*, *SIGMAR1*, and *YES1* (Figure 6A). We assessed further the influences of miR-193a-5p mimics

on the expression levels of potential target genes by RT-qPCR. We established that miR-193a-5p mimics remarkably down-regulated the mRNA level of *YES1* (Figure 6B). In addition, the Western blotting data

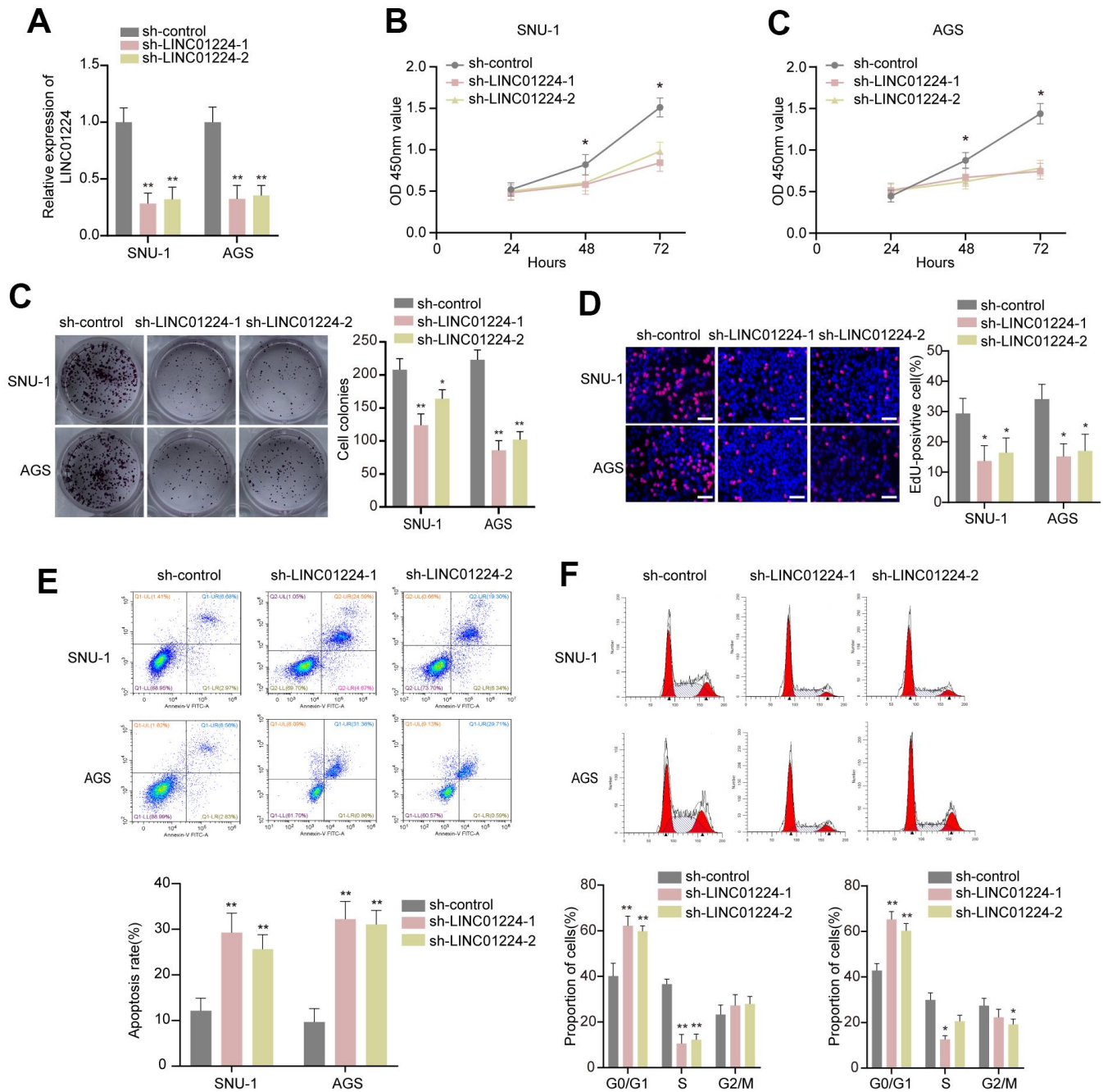


Figure 3. Effect of LINC01224 on the biological behavior of gastric cancer cells *in vitro*. (A) LINC01224 expression was knocked down by two shRNAs targeting LINC01224 in SNU-1 and AGS cells. (B) CCK-8 assay found that knockdown of LINC01224 significantly decreased the proliferation of AGS and SNU-1 cells compared with sh-control. (C) The colony numbers of SNU-1 and AGS cells transfected with sh-LINC01224 were significantly lower than those transfected with sh-control. (D) EdU assay showed that knockdown of LINC01224 inhibited the proliferation of SNU-1 and AGS cells. Scale bars = 50 μ m. (E) Flow cytometry assay found that knockdown of LINC01224 promoted apoptosis of SNU-1 and AGS cells by Annexin V-PI staining. (F) Flow cytometry analysis of cell cycle distribution showed that the number of SNU-1 and AGS cells arrested in the G1 phase was significantly increased after knockdown of LINC01224.

illustrated that the protein expression level of *YES1* was also drastically down-regulated by miR-193a-5p mimics (Figure 6C). The data of the dual-luciferase enzyme reporter assay exhibited that miR-193a-5p mimics drastically decreased the luciferase enzyme activity containing wild-type 3'-UTR segment of *YES1* plasmid rather than mutant-3'-UTR segment of *YES1* plasmid

(Figure 6D). Overexpression of wt-LINC01224 could partially eliminate the repressive influences of miR-193a-5p mimics on the luciferase enzyme activity of plasmid harboring wild-type 3'-UTR segment of *YES1* (Figure 6E). Besides, overexpression of wt-LINC01224 could partially reverse the inhibition of the *YES* expression level by miR-193a-5p mimics (Figure 6F).

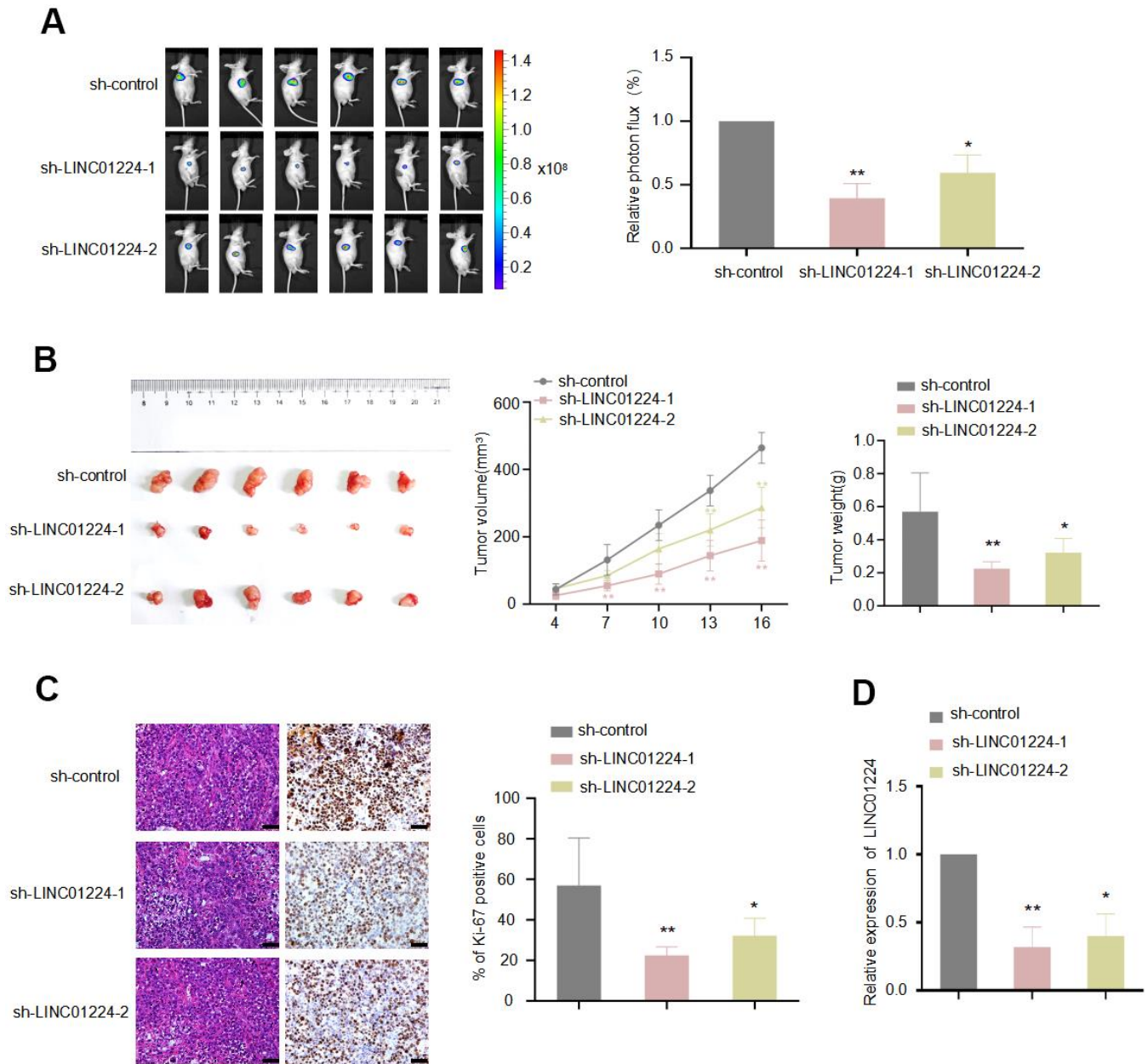


Figure 4. LINC01224 regulates the growth of gastric cancer cells *in vivo*. Nude mice were subcutaneously transplanted with AGS-Luc2 cells transfected with LINC01224 shRNA or control shRNA. 16 days later, mice were sacrificed. **(A)** IVIS images showed the effect of knockdown of LINC01224 on the growth of xenografts in nude mice. Mice were imaged for bioluminescence. **(B)** The left image shows the morphology of the xenograft tumor after 16 days of implantation. The middle chart shows the change in graft volume every 3 days after injection. The right chart shows the weight of the transplanted tumor after 16 days of injection. **(C)** Ki-67 staining of transplanted tumor after knockdown of LINC01224. Scale bars = 50 μ m. **(D)** The effect of shRNA on LINC01224 mRNA expression of xenograft tumor in nude mice was detected by qRT-PCR.

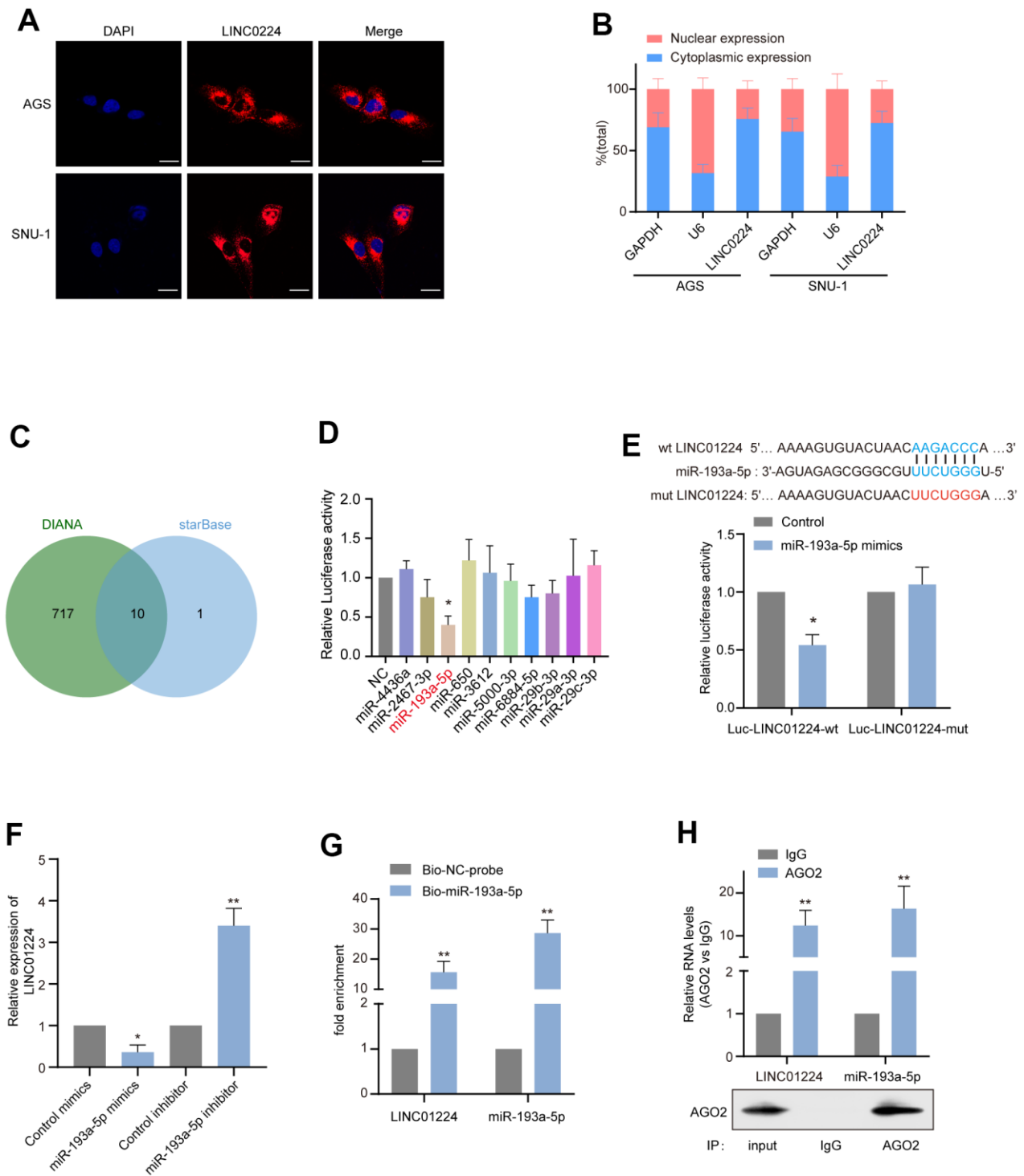


Figure 5. LINC0224 acts as the molecular sponge of miR-193a-5p in gastric cancer cells. (A) The subcellular location of LINC0224 (red) in AGS and SNU-1 was detected by FISH. The nuclei were stained with DAPI (blue). Scale bar = 10 μ m. (B) The relative expression level of LINC0224 in the nucleus and cytoplasm of AGS and SNU-1 cells. Nuclear control: U6; cytoplasmic control: GAPDH. (C) Venn diagram of overlapping target miRNAs predicted using the DIANA and starBase online analysis tools. (D) Dual-luciferase reporter assay was used to determine the direct targeting miRNAs of LINC0224. (E) Dual-luciferase reporter assays were performed with wild-type and mutant-type luciferase reporter vectors (mutations occurring at sites that may bind to miR-193a-5p). (F) Effects of overexpression and inhibition of miR-193a-5p on mRNA expression of LINC0224. (G) LINC0224 and miR-193a-5p were highly enriched in samples pulled down by biotinylated miR-193a-5p rather than control probes. (H) RNA immunoprecipitation with anti-Ago2 antibody was used to detect the binding of LINC0224 and miR-193a-5p to endogenous Ago2, and IgG was used as a control. LINC0224 and miR-193a-5p levels were determined by qRT-PCR and expressed as fold enrichment relative to the input Ago2. RIP efficiency of Ago2 protein was detected by Western blot.

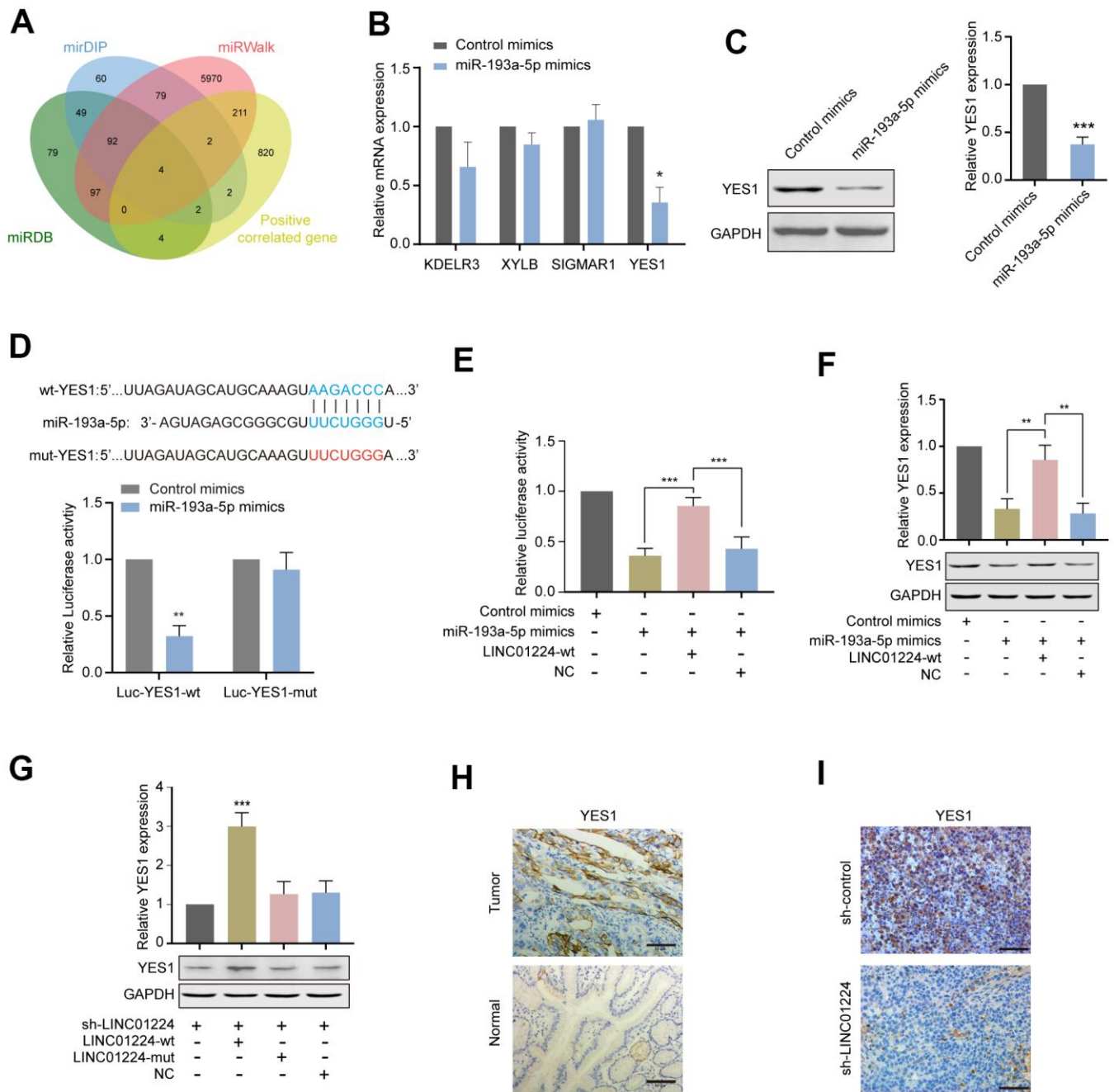


Figure 6. LINC01224 regulates the expression of YES1, a target gene of miR-193a-5p. (A) Prediction of potential genes competing with LINC01224 for adsorption of miR-193a-5p. We first use the online websites (miRDB, miRIP and miRWalk) to predict the target genes of miR-193a-5p, and then intersect with the co-expressed genes of LINC01224 to obtain the potential target genes of LINC01224. (B) The effect of miR-193a-5p mimics on the expression of potential target genes was detected by qRT-PCR. (C) Western blot analysis of YES1 expression in AGS cells by overexpressing miR-193a-5p. (D) Dual-luciferase reporter assay showed that miR-193a-5p mimics significantly decreased the luciferase activity containing wild-type 3'-UTR segment of YES1 plasmid rather than mutant-3'-UTR segment of YES1 plasmid. (E) Dual-luciferase reporter assay showed that overexpression of wt-LINC01224 could partially eliminate the inhibitory effects of miR-193a-5p mimics on the luciferase activity of plasmid containing wild-type 3'-UTR segment of YES1. (F) Western blot showed that miR-193a-5p mimics decreased YES1 expression, while overexpression of LINC01224 partially reversed the inhibition of YES1 expression by miR-193a-5p mimics. (G) Western blot showed that wild-type LINC01224 enhanced YES1 expression, whereas the mutated LINC01224 containing a mutation in the binding site of miR-193a-5p could not increase YES1 expression. (H) Immunohistochemical staining showed that YES1 was highly expressed in gastric cancer compared with paracancerous tissues. Scale bar = 50 μ m. (I) Immunohistochemical staining showed that YES1 expression was significantly decreased in xenografts with LINC01224 knockdown compared with control tissues. Scale bar = 50 μ m.

To clarify whether the miR-193a-5p docking site on LINC01224 is the key to modulate *YES1* expression level, we silenced the expression level of endogenous LINC01224, and then, transfected cells with the wt-LINC01224 plasmid and a mut-LINC01224 plasmid containing mutant miR-193a-5p docking site. We found that the wt-LINC01224 plasmid, rather than the mut-LINC01224 plasmid, could drastically up-regulate the expression level of *YES1* (Figure 6G). Moreover, *YES1* was over-expressed in GC tissues in comparison with non-malignant tissues (Figure 6H). *YES1* expression level in the LINC01224-knockdown group was drastically reduced in comparison with that in the control group (Figure 6D). Taken together, LINC01224 showed to act as a ceRNA in GC cells to promote *YES1* level of expression by adsorbing miR-193a-5p.

LINC01224 regulated the cell cycle, proliferation, along with apoptosis of GC cells by acting as a ceRNA to compete with *YES1*

In order to study whether could LINC01224 works as a ceRNA to modulate the cell cycle, proliferation, colony formation, along with the apoptosis of GC cells, we transfected a mut-LINC01224 plasmid with a mutation at the miR-193a-5p docking site, the wt-LINC01224 plasmid, an miR-193a-5p inhibitor, and a *YES1*-overexpressing plasmid into AGS cells. The results of CCK8 data illustrated that the miR-193a-5p inhibitor, *YES1*-overexpressing plasmid, and wt-LINC01224 plasmid partially reversed the repressive influence of silencing of LINC01224 on the proliferation of AGS cells, whereas the mut-LINC01224 plasmid could not ($P < 0.05$, Figure 7A). Colony formation ($P < 0.05$, Figure 7B, 7C) and EdU ($P < 0.05$, Figure 7D, 7E) assays illustrated that the miR-193a-5p inhibitor, *YES1*-overexpressing plasmid, and wt-LINC01224 plasmid attenuated the growth arrest of AGS cells caused by the knockdown of LINC01224, while the mut-LINC01224 plasmid could not. The results of flow cytometry indicated that the miR-193a-5p inhibitor, *YES1*-overexpressing plasmid, and wt-LINC01224 plasmid partially reversed the apoptosis ($P < 0.05$, Figure 7F, 7G) and G1 phase cell cycle arrest ($P < 0.05$, Figure 7H, 7I) of AGS cells caused by the knockdown of LINC01224, whereas the mut-LINC01224 plasmid could not. The above-mentioned results strongly suggested that the repression of proliferation, G1 phase cell cycle arrest, as well as apoptosis of GC cells by silencing of LINC01224 were partially regulated by the miR-193a-5p/*YES1* axis.

DISCUSSION

Although the diagnosis and treatment of GC have notably attracted scholars' attention in recent decades,

GC still ranks among the top 10 causes of cancer-linked deaths in the world [19]. It is therefore of great clinical importance to find out the key molecules affecting the progression of GC. LncRNAs have been proven to be linked to the progress of diverse kinds of cancer, for instance, gastric cancer [20], prostate cancer [21], and breast cancer [22]. LINC01224 was documented to be over-expressed in ovarian cancer, and it was linked to the tumor size, tumor stage, along with lymph node metastasis [17]. LINC01224 was also documented to be expressed highly in hepatocellular carcinoma cells and was also linked to the TNM stage along with distant metastasis [5]. However, the relationship of the expression level of LINC01224 with the progress of GC has not been documented. We established that the expression level of LINC01224 was drastically upregulated in GC cells by analyzing data from the TCGA and GTEx databases. We also noted that the expression of LINC01224 was markedly elevated in GC tissues, as well as cell lines. The high expression level of LINC01224 was remarkably linked to the depth of tumor invasion and TNM stage. The prognosis of individuals with GC elevated expression of LINC01224 was poor. Univariate along with the multivariate regression analyses illustrated that the LINC01224 could be an independent risk factor GC prognosis.

Growing research evidence documents that lncRNAs could enhance the onset and progress of cancer cells by regulating diverse biological behaviors, such as the cell growth, apoptosis, cell cycle, migration, along with invasion. LINC01224 promotes the cell growth, migration, as well as invasion, and inhibits the apoptosis of ovarian cancer cells [17]. It also enhances the growth of hepatoma cells *in vitro* and *in vivo* [5]. Nonetheless, it is not clear whether LINC01224 has similar biological functions in GC. We created a co-expression network of LINC01224 by the correlation analysis, and found that LINC01224 was correlated to the proliferation, DNA replication, along with cell cycle of GC cells by the GO along with KEGG analyses. Similar results were obtained from the GSEA. We established that knockdown of LINC01224 inhibited the cell growth, as well as triggered the apoptosis of GC cells. *In vivo* assays illustrated silencing of LINC01224 repressed GC cell growth in nude mice. In summary, LINC01224 serves as a tumor-enhancing factor in GC.

LncRNAs may modulate the transcription along with the translation of adjacent and distant genes through cis- and trans-modulatory functions [23]. It has been documented that lncRNAs can act as ceRNA sponges for miRNAs to release protein-coding genes to regulate the occurrence and development of cancer [24]. LINC01224 has been documented to control the malignant behavior of ovarian cancer cells by adsorbing

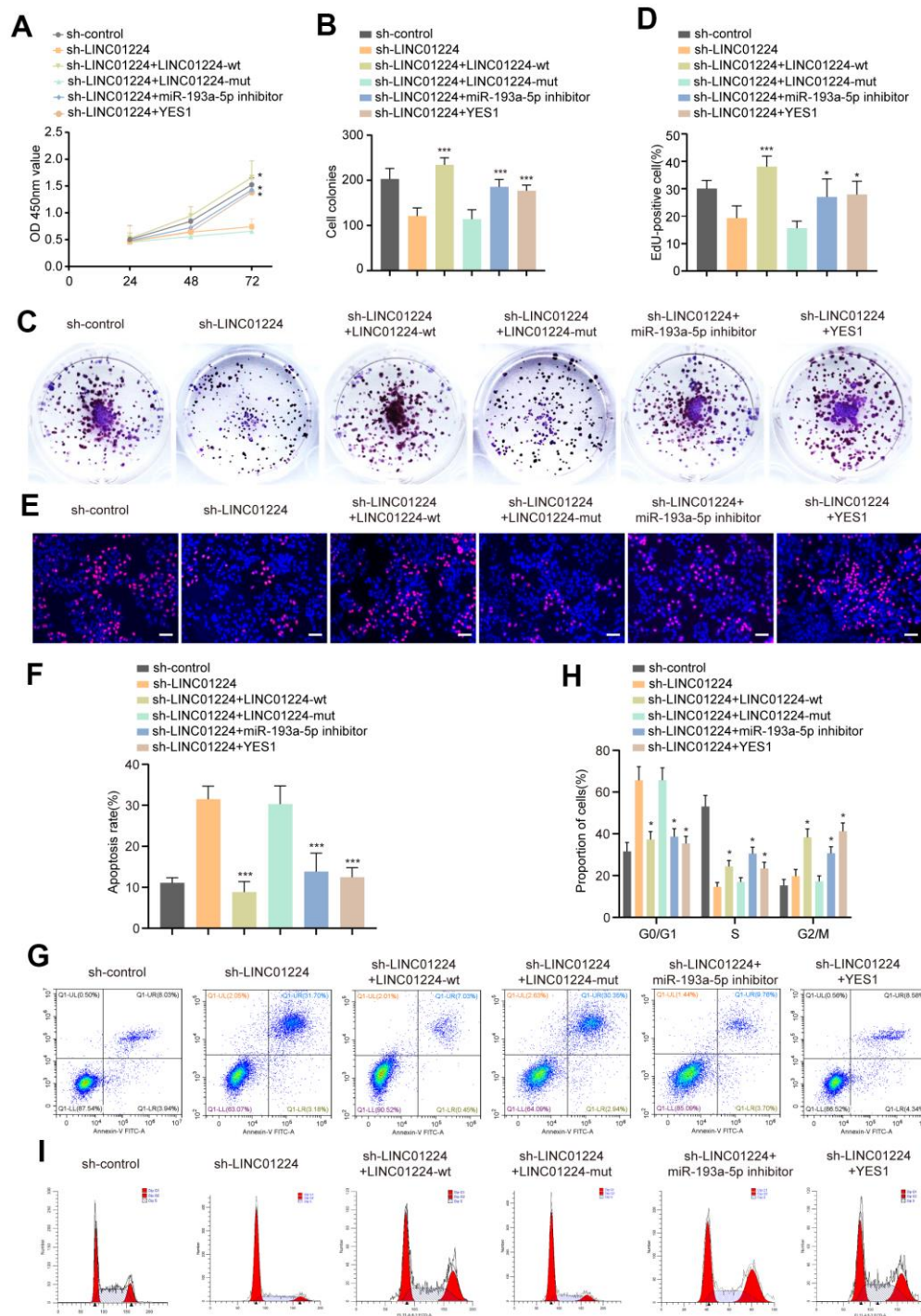


Figure 7. LINC01224 regulates the proliferation, cycle and apoptosis by competing with YES1 for binding to miR-193a-5p. (A) CCK8 showed that the miR-193a-5p inhibitor, YES1-overexpressing plasmid, and wt-LINC01224 plasmid partially reversed the inhibitory effect of silencing of LINC01224 on the proliferation of AGS cells, whereas the mut-LINC01224 plasmid could not. (B, C) Colony formation assays showed that the miR-193a-5p inhibitor, YES1-overexpressing plasmid, and wt-LINC01224 plasmid attenuated the growth arrest of AGS cells caused by the knockdown of LINC01224, while the mut-LINC01224 plasmid could not. (D, E) EDU experiments showed that the miR-193a-5p inhibitor, YES1-overexpressing plasmid, and wt-LINC01224 plasmid attenuated the growth arrest of AGS cells caused by the knockdown of LINC01224, while the mut-LINC01224 plasmid could not. Scale bars = 50 μ m. (F, G) Flow cytometry assays showed that the miR-193a-5p inhibitor, YES1-overexpressing plasmid, and wt-LINC01224 plasmid partially reversed the apoptosis of AGS cells caused by the knockdown of LINC01224, whereas the mut-LINC01224 plasmid could not. (H, I) Flow cytometry assays showed that the miR-193a-5p inhibitor, YES1-overexpressing plasmid, and wt-LINC01224 plasmid partially reversed the G1 phase cell cycle arrest of AGS cells caused by the knockdown of LINC01224, whereas the mut-LINC01224 plasmid could not.

microRNA-485-5p [17]. The expression level of LINC01224 is up-regulated in hepatocellular carcinoma cells, and it absorbs microRNA-330-5p as a sponge to enhance the progress of hepatocellular carcinoma [5]. Bioinformatics analysis suggested that the potential miRNA interacting with LINC01224 may be miR-193a-5p. Dual-luciferase enzyme reporter, RNA pull-down, and RIP assays validated that LINC01224 could directly dock to miR-193a-5p. The results of the functional experiments showed that the effects caused by the knockdown of LINC01224 could be partially reverted by an miR-193a-5p inhibitor. To further confirm that LINC01224 could modulate the growth of GC cells by binding to miR-193a-5p, we first silenced the expression level of LINC01224 in GC cells, and then, transfected the wt-LINC0224 and mut-LINC0224 plasmids, respectively, into these cells. We found that the transfection of wt-LINC0224 could reverse the growth of GC cells induced by knockdown of LINC01224, whereas mut-LINC01224 could not. These data illustrated that LINC01224 could modulate the growth of GC cells in a miR-193a-5p-dependent manner.

A miRNA may simultaneously regulate multiple target genes, while only genes that have a ceRNA-dependent relationship with LINC01224 were investigated herein. miR-193a-5p's target genes in GC have still remained unknown, thus, we used some online tools to predict its target genes. We speculate that LINC01224 shares similar expression patterns with its target genes according to the ceRNA theory. Therefore, we carried out co-expression analysis, then, intersected the co-expression genes of LINC01224 with the potential miR-193a-5p's target genes, and obtained four target genes, including *YES1*. We confirmed that *YES1* was the target gene of miR-193a-5p by the dual-luciferase enzyme reporter assay. To further clarify the ceRNA-dependent relationship between *YES1* and LINC01224, we first knocked down LINC01224 and then found that the transfection of wt-LINC01224, rather than the transfection of mut-LINC01224, could drastically up-regulate the expression level of *YES1*. We confirmed that there was a ceRNA-dependent relationship between *YES1* and LINC01224 through a series of experiments. *YES1* is a non-receptor protein-tyrosine kinase that interacts with receptor-tyrosine kinases, such as EGFR, PDGFR, and CDF1R, and it participates in regulating the cell growth, apoptosis, and cell cycle. *YES1* has been documented to be over-expressed in non-small cell lung cancer [25] and esophageal cancer [26], and is linked to a dismal prognosis of individuals with these cancers. Fang et al. [27] documented that miR-140-5p blocked the growth, migration, along with the infiltration of GC cells by targeting *YES1*. We, in the present research, found that overexpression of *YES1*

partially reverted the repressive influences of knocking down LINC01224, as well as miR-193a-5p inhibitor on the growth of GC cells. In conclusion, there is a ceRNA-dependent relationship among LINC01224, miR-193a-5p, and *YES1*, which regulates the malignant progression of GC cells.

CONCLUSIONS

In summary, our findings suggested that LINC01224 was highly expressed in GC tissues and cell lines, and it was linked to a poor prognosis of individuals with GC. LINC01224 exhibited to modulate the growth along with the apoptosis of GC cells by competing with *YES1* to adsorb miR-193a-5p. Therefore, the LINC01224/miR-193a-5p/*YES1* axis is a prospective diagnostic, as well as therapeutic target for GC.

AUTHOR CONTRIBUTIONS

Conception and design: Yansong Pu, Fei Xue, Jianhua Wang; Development of methodology: Qingguo Du, Yu Ma, Yansong Pu, Yi Liu; Acquisition of data (acquired and managed patients, provided facilities, etc.): Baojun Duan, Min Wu, Yansong Pu; Analysis and interpretation of data (e.g., statistical analysis, biostatistics, computational analysis): Yanbin Long, Jianhua Wang, Yi Liu; Writing, review, and/or revision of the manuscript: Yansong Pu, Fei Xue; Study supervision: Yi Liu.

ACKNOWLEDGMENTS

This manuscript was edited by a prestigious company, TopEdit (www.topeditsci.com), professionally working on English language editing services.

CONFLICTS OF INTEREST

The authors declare that they have no conflicts of interest.

FUNDING

This study was supported by scientific and technological project of Xi'an [2017113SF/YX007(11)], Shaanxi Provincial Project of Scientific and Technological Innovation Team (2017KCT-28) and Shaanxi Natural Science Foundation (2020JQ-947), NSFC (8142012), Shaanxi Natural Science Foundation (2015JQ8321), Shaanxi Natural Science Foundation (2019JM-547), Operating Expenses of Basic Scientific Research Project of Xi'an Jiaotong University (xzy012019112), scientific and technological project of Xi'an [(2019114613YX001SF035(3)].

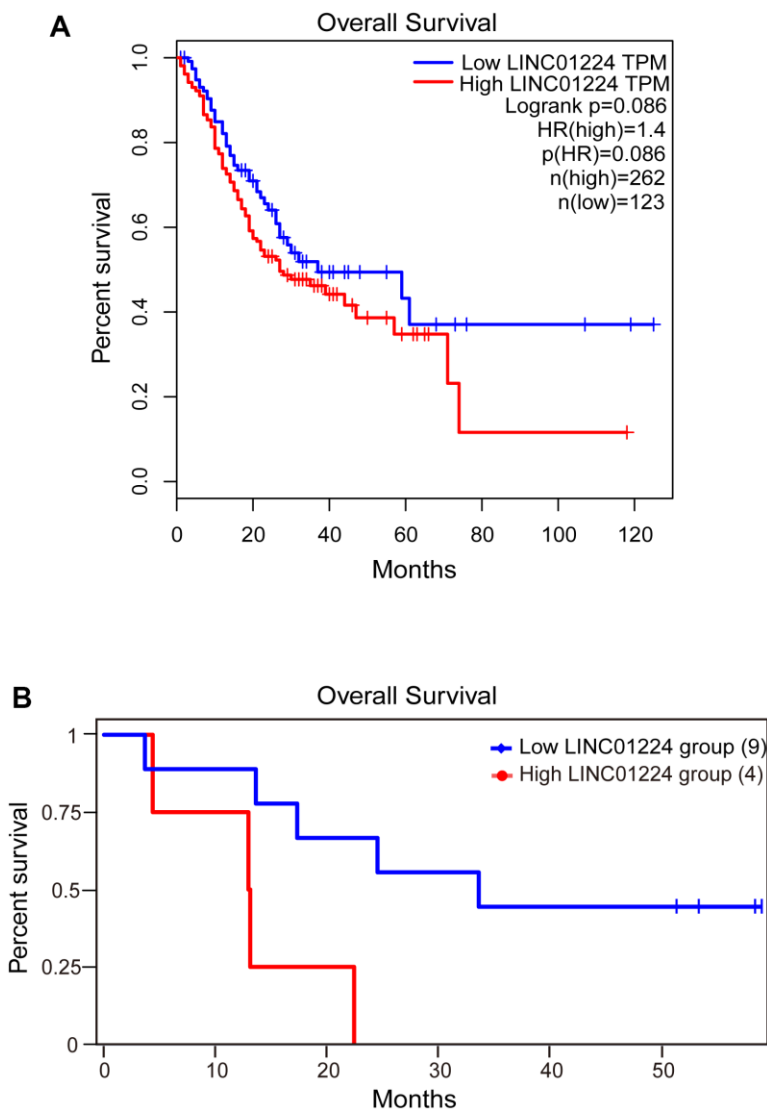
REFERENCES

1. Bray F, Ferlay J, Soerjomataram I, Siegel RL, Torre LA, Jemal A. Global cancer statistics 2018: GLOBOCAN estimates of incidence and mortality worldwide for 36 cancers in 185 countries. *CA Cancer J Clin.* 2018; 68:394–424.
<https://doi.org/10.3322/caac.21492>
PMID:[30207593](https://pubmed.ncbi.nlm.nih.gov/30207593/)
2. Qian B, Yao Z, Yang Y, Li N, Wang Q. Downregulation of SDCBP inhibits cell proliferation and induces apoptosis by regulating PI3K/AKT/mTOR pathway in gastric carcinoma. *Biotechnol Appl Biochem.* 2021. [Epub ahead of print].
<https://doi.org/10.1002/bab.2103> PMID:[33432665](https://pubmed.ncbi.nlm.nih.gov/33432665/)
3. Evans JR, Feng FY, Chinnaiyan AM. The bright side of dark matter: lncRNAs in cancer. *J Clin Invest.* 2016; 126:2775–82.
<https://doi.org/10.1172/JCI84421> PMID:[27479746](https://pubmed.ncbi.nlm.nih.gov/27479746/)
4. Leucci E. Cancer development and therapy resistance: spotlights on the dark side of the genome. *Pharmacol Ther.* 2018; 189:22–30.
<https://doi.org/10.1016/j.pharmthera.2018.04.001>
PMID:[29649500](https://pubmed.ncbi.nlm.nih.gov/29649500/)
5. Gong D, Feng PC, Ke XF, Kuang HL, Pan LL, Ye Q, Wu JB. Silencing Long Non-coding RNA LINC01224 Inhibits Hepatocellular Carcinoma Progression via MicroRNA-330-5p-Induced Inhibition of CHEK1. *Mol Ther Nucleic Acids.* 2020; 19:482–97.
<https://doi.org/10.1016/j.omtn.2019.10.007>
PMID:[31902747](https://pubmed.ncbi.nlm.nih.gov/31902747/)
6. Li H, Gao C, Liu L, Zhuang J, Yang J, Liu C, Zhou C, Feng F, Sun C. 7-lncRNA Assessment Model for Monitoring and Prognosis of Breast Cancer Patients: Based on Cox Regression and Co-expression Analysis. *Front Oncol.* 2019; 9:1348.
<https://doi.org/10.3389/fonc.2019.01348>
PMID:[31850229](https://pubmed.ncbi.nlm.nih.gov/31850229/)
7. Marchese FP, Raimondi I, Huarte M. The multidimensional mechanisms of long noncoding RNA function. *Genome Biol.* 2017; 18:206.
<https://doi.org/10.1186/s13059-017-1348-2>
PMID:[29084573](https://pubmed.ncbi.nlm.nih.gov/29084573/)
8. Tay Y, Rinn J, Pandolfi PP. The multilayered complexity of ceRNA crosstalk and competition. *Nature.* 2014; 505:344–52.
<https://doi.org/10.1038/nature12986> PMID:[24429633](https://pubmed.ncbi.nlm.nih.gov/24429633/)
9. Karreth FA, Pandolfi PP. ceRNA cross-talk in cancer: when ce-bling rivalries go awry. *Cancer Discov.* 2013; 3:1113–21.
<https://doi.org/10.1158/2159-8290.CD-13-0202>
PMID:[24072616](https://pubmed.ncbi.nlm.nih.gov/24072616/)
10. Chen J, Gao S, Wang C, Wang Z, Zhang H, Huang K, Zhou B, Li H, Yu Z, Wu J, Chen C. Pathologically decreased expression of miR-193a contributes to metastasis by targeting WT1-E-cadherin axis in non-small cell lung cancers. *J Exp Clin Cancer Res.* 2016; 35:173.
<https://doi.org/10.1186/s13046-016-0450-8>
PMID:[27821145](https://pubmed.ncbi.nlm.nih.gov/27821145/)
11. Khordadmehr M, Shahbazi R, Sadreddini S, Baradaran B. miR-193: A new weapon against cancer. *J Cell Physiol.* 2019; 234:16861–72.
<https://doi.org/10.1002/jcp.28368> PMID:[30779342](https://pubmed.ncbi.nlm.nih.gov/30779342/)
12. Ma J, Han LN, Song JR, Bai XM, Wang JZ, Meng LF, Li J, Zhou W, Feng Y, Feng WR, Ma JJ, Hao JT, Shen ZQ. Long noncoding RNA LINC01234 silencing exerts an anti-oncogenic effect in esophageal cancer cells through microRNA-193a-5p-mediated CCNE1 downregulation. *Cell Oncol (Dordr).* 2020; 43:377–94.
<https://doi.org/10.1007/s13402-019-00493-5>
PMID:[32130660](https://pubmed.ncbi.nlm.nih.gov/32130660/)
13. Tang Z, Li C, Kang B, Gao G, Li C, Zhang Z. GEPIA: a web server for cancer and normal gene expression profiling and interactive analyses. *Nucleic Acids Res.* 2017; 45:W98–102.
<https://doi.org/10.1093/nar/gkx247> PMID:[28407145](https://pubmed.ncbi.nlm.nih.gov/28407145/)
14. Hu X, Qiu Z, Zeng J, Xiao T, Ke Z, Lyu H. A novel long non-coding RNA, AC012456.4, as a valuable and independent prognostic biomarker of survival in oral squamous cell carcinoma. *PeerJ.* 2018; 6:e5307.
<https://doi.org/10.7717/peerj.5307> PMID:[30128179](https://pubmed.ncbi.nlm.nih.gov/30128179/)
15. Liu W, Luo W, Zhou P, Cheng Y, Qian L. Bioinformatics Analysis and Functional Verification of ADAMTS9-AS1/AS2 in Lung Adenocarcinoma. *Front Oncol.* 2021; 11:681777.
<https://doi.org/10.3389/fonc.2021.681777>
PMID:[34395250](https://pubmed.ncbi.nlm.nih.gov/34395250/)
16. Li JH, Liu S, Zhou H, Qu LH, Yang JH. starBase v2.0: decoding miRNA-ceRNA, miRNA-ncRNA and protein-RNA interaction networks from large-scale CLIP-Seq data. *Nucleic Acids Res.* 2014; 42:D92–97.
<https://doi.org/10.1093/nar/gkt1248> PMID:[24297251](https://pubmed.ncbi.nlm.nih.gov/24297251/)
17. Xing S, Zhang Y, Zhang J. LINC01224 Exhibits Cancer-Promoting Activity in Epithelial Ovarian Cancer Through microRNA-485-5p-Mediated PAK4 Upregulation. *Onco Targets Ther.* 2020; 13:5643–55.
<https://doi.org/10.2147/OTT.S254662> PMID:[32606778](https://pubmed.ncbi.nlm.nih.gov/32606778/)
18. Hutvagner G, Simard MJ. Argonaute proteins: key players in RNA silencing. *Nat Rev Mol Cell Biol.* 2008; 9:22–32.
<https://doi.org/10.1038/nrm2321> PMID:[18073770](https://pubmed.ncbi.nlm.nih.gov/18073770/)
19. Siegel RL, Miller KD, Jemal A. Cancer statistics, 2020. *CA Cancer J Clin.* 2020; 70:7–30.

- <https://doi.org/10.3322/caac.21590>
PMID:[31912902](https://pubmed.ncbi.nlm.nih.gov/31912902/)
20. Zhu X, Tian X, Yu C, Shen C, Yan T, Hong J, Wang Z, Fang JY, Chen H. A long non-coding RNA signature to improve prognosis prediction of gastric cancer. *Mol Cancer*. 2016; 15:60.
<https://doi.org/10.1186/s12943-016-0544-0>
PMID:[27647437](https://pubmed.ncbi.nlm.nih.gov/27647437/)
21. Xu YH, Deng JL, Wang G, Zhu YS. Long non-coding RNAs in prostate cancer: Functional roles and clinical implications. *Cancer Lett*. 2019; 464:37–55.
<https://doi.org/10.1016/j.canlet.2019.08.010>
PMID:[31465841](https://pubmed.ncbi.nlm.nih.gov/31465841/)
22. Amelio I, Bernassola F, Candi E. Emerging roles of long non-coding RNAs in breast cancer biology and management. *Semin Cancer Biol*. 2021; 72:36–45.
<https://doi.org/10.1016/j.semcancer.2020.06.019>
PMID:[32619506](https://pubmed.ncbi.nlm.nih.gov/32619506/)
23. Yan P, Luo S, Lu JY, Shen X. Cis- and trans-acting lncRNAs in pluripotency and reprogramming. *Curr Opin Genet Dev*. 2017; 46:170–78.
<https://doi.org/10.1016/j.gde.2017.07.009>
PMID:[28843809](https://pubmed.ncbi.nlm.nih.gov/28843809/)
24. Zhou Q, Chen F, Zhao J, Li B, Liang Y, Pan W, Zhang S, Wang X, Zheng D. Long non-coding RNA PVT1 promotes osteosarcoma development by acting as a molecular sponge to regulate miR-195. *Oncotarget*. 2016; 7:82620–33.
<https://doi.org/10.18632/oncotarget.13012>
PMID:[27813492](https://pubmed.ncbi.nlm.nih.gov/27813492/)
25. Garmendia I, Pajares MJ, Hermida-Prado F, Ajona D, Bértolo C, Sainz C, Lavín A, Remírez AB, Valencia K, Moreno H, Ferrer I, Behrens C, Cuadrado M, et al. YES1 Drives Lung Cancer Growth and Progression and Predicts Sensitivity to Dasatinib. *Am J Respir Crit Care Med*. 2019; 200:888–99.
<https://doi.org/10.1164/rccm.201807-1292OC>
PMID:[31166114](https://pubmed.ncbi.nlm.nih.gov/31166114/)
26. Hamanaka N, Nakanishi Y, Mizuno T, Horiguchi-Takei K, Akiyama N, Tanimura H, Hasegawa M, Satoh Y, Tachibana Y, Fujii T, Sakata K, Ogasawara K, Ebiike H, et al. YES1 Is a Targetable Oncogene in Cancers Harboring YES1 Gene Amplification. *Cancer Res*. 2019; 79:5734–45.
<https://doi.org/10.1158/0008-5472.CAN-18-3376>
PMID:[31391186](https://pubmed.ncbi.nlm.nih.gov/31391186/)
27. Fang Z, Yin S, Sun R, Zhang S, Fu M, Wu Y, Zhang T, Khaliq J, Li Y. miR-140-5p suppresses the proliferation, migration and invasion of gastric cancer by regulating YES1. *Mol Cancer*. 2017; 16:139.
<https://doi.org/10.1186/s12943-017-0708-6>
PMID:[28818100](https://pubmed.ncbi.nlm.nih.gov/28818100/)

SUPPLEMENTARY MATERIALS

Supplementary Figures



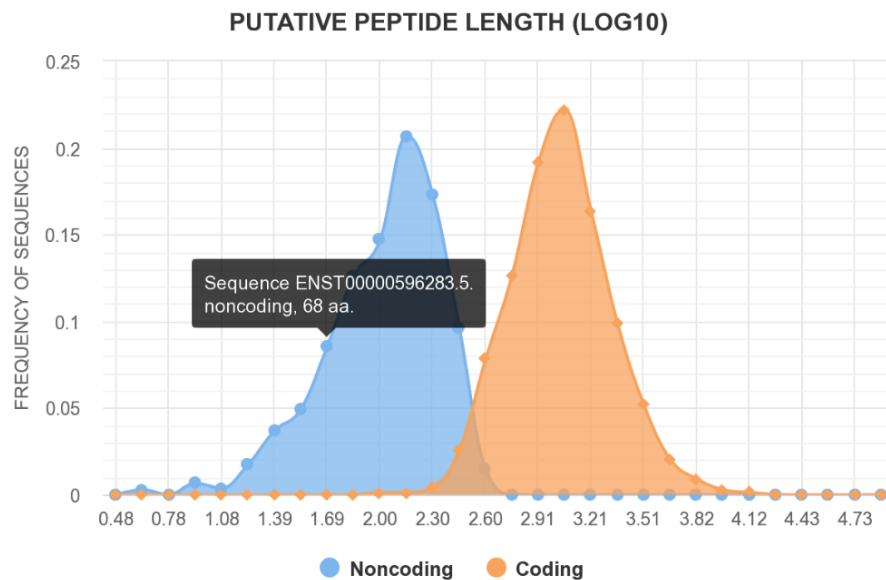
Supplementary Figure 1. The correlation between the expression level of LINC01224 and OS of GC patients. (A) The OS rate of GC patients in the high LINC01224 expression group was lower than that of patients in the low LINC01224 expression group that analyzed the TCGA database using the GEPIA. (B) The analysis of GSE38749 dataset performed using the InCAR website indicated that GC patients in the high LINC01224 expression group had a lower OS rate than those in the low LINC01224 expression group.

A

Data ID	Sequence Name	RNA Size	ORF Size	Fickett Score	Hexamer Score	Coding Probability	Coding Label
0	ENST00000596283.5	2766	204	0.6975	-0.480418477445	0.00087563467139802	no
1	LINC01224-203	194	6	0.3194	-3.34444417906	2.2520034605241E-13	no
2	LINC01224-203	106	6	0.6163	0.754487205573	0.24589743023214	no
3	LINC01224-203	78	36	0.7387	-0.451578417299	0.00023097401553011	no
4	LINC01224-203	158	48	0.8568	-0.191563923545	0.0021071812229215	no
5	LINC01224-203	28	9	0.7426	0.5763771108	0.13440296780496	no
6	LINC01224-203	288	57	0.8583	-0.044335325539	0.0060954366506059	no
7	LINC01224-203	336	66	0.4147	-0.191843738299	0.00063111150515418	no
8	LINC01224-203	1578	204	0.6975	-0.480418477445	0.00094106959004621	no
9	LINC01224-203	1792	147	0.7585	-0.24959196441	0.0027838498039605	no
10	LINC01224-203	664	192	0.7466	-0.374857558437	0.0020444802640556	no
11	LINC01224-203	149	6	0.3299	-2.90185301361	4.3368286332487E-12	no
12	LINC01224-203	1203	207	0.4736	-0.241649972359	0.0023773854266959	no
13	LINC01224-203	226	0	0	0	0.00030024298547403	no
14	LINC01224-203	693	81	0.6674	-0.397629793384	0.00041301298044843	no
15	LINC01224-203	1129	192	0.8405	-0.320245573025	0.0038218286929068	no

B

Sequence ENST00000596283.5 got Fickett score 0.28007 with a complete putative ORF 68 AA, a pI 7.71917724609, which, in total, classify it as a noncoding sequence with coding probability 0.0321526.



Supplementary Figure 2. The prediction of the protein-coding ability of LINC01224. (A) The predicted results of CPAT website indicated that the transcript ENST00000596283.5 of LINC01224 had no protein-coding ability. (B) The CPC website's predicted results indicated that the transcript ENST00000596283.5 of LINC01224 is a noncoding sequence with coding probability 0.0321526.

Supplementary Table

Supplementary Table 1. The list of primers and sh-RNAs sequence.

	Forward	Reverse
LINC01224	5'-ACGTGCACAGACAGCTAAGA-3'	5'-ATCATCCACGGGAGTGACGA-3'
YES1	5'-TTGGAGGTGCATCTTCCTC-3'	5'-CCACAAATATAGTAACACCACCTG-3'
KDEL3	5'-CACTCTGCTGGAGATCCTC-3'	5'-TTGCTGATCATGAAGAGCT-3'
XYLB	5'-TTCGAGCACTAATTGAAGGAC-3'	5'-TTGCTTTGGACATGACTCG-3'
SIGMAR1	5'-GAAGAGATAGCGCAGTTGG-3'	5'-CTCCACGATCAGACGAGAG-3'
GAPDH	5'-TCAAGATCATCAGCAATGCC-3'	5'-CGATACCAAAGTTGTCATGGA-3'
U6	5'-ATACAGAGAAAGTTAGCACGG-3'	5'-GGAATGCTTCAAAGAGTTGTG-3'
miR-4436a	5'-ATGGCAGGACAGGCAGAAG-3'	5'-GTCGTATCCAGTGCAGGGTC-3'
miR-2467-3p	5'-TCGAGCAGAGGCAGAGAGG-3'	5'-GTCGTATCCAGTGCAGGGTC-3'
miR-193a-5p	5'-GGTCTTTGCGGGCGAGATG-3'	5'-GTCGTATCCAGTGCAGGGTC-3'
miR-650	5'-TAGGAGGCAGCGCTCTCAG-3'	5'-GTCGTATCCAGTGCAGGGTC-3'
miR-3612	5'-CTAGCGAGGAGGCATCTTGAG-3'	5'-GTCGTATCCAGTGCAGGGTC-3'
miR-5000-3p	5'-CGCGTCAGGACACTTCTGAAC-3'	5'-GTCGTATCCAGTGCAGGGTC-3'
miR-6884-5p	5'-TGCGAGAGGCTGAGAAGGT-3'	5'-GTCGTATCCAGTGCAGGGTC-3'
miR-29b-3p	5'-TCCGTAGCACCATTTGAAATCAG-3'	5'-GTCGTATCCAGTGCAGGGTC-3'
miR-29a-3p	5'-CGCGTAGCACCATCTGAAATCG-3'	5'-GTCGTATCCAGTGCAGGGTC-3'
miR-29c-3p	5'-CGCGTAGCACCATTTGAAATCG-3'	5'-GTCGTATCCAGTGCAGGGTC-3'
sh-LINC01224-1	5'-CCGGTACTCTCCTGCCTGGATTTAACTCGAG TTAAATCCAGGCAGGAGAGTATTTTTG-3'	5'-AATTCAAAAATACTCTCCTGCCTGGA TTTAACTCGAGTTAAATCCAGGCAGGAGAG TA-3'
sh-LINC01224-2	5'-CCGGGATCAAAGGCGCCTGTAATTTCTCGAGAA ATTACAGGCGCCTTTGATCTTTTTG-3'	5'-AATTCAAAAAGATCAAAGGCGCCTG TAATTTCTCGAGAAATTACAGGCGCCTTTG ATC-3'
sh-YES1	5'-CCGGGCTGATGGTATGGCATATATTCAAGAG ATATATGCCATACCATCAGCTTTTTTG-3'	5'-AATTCAAAAAGCTGATGGTATGGCA TATATCTTTGAATATATGCCATACCATCA GC-3'
sh-control	5'-CCGGTTCTCCGAACGTGTCACGTTTCAAGAGAA CGTGACACGTTCCGAGAATTTTTTG-3'	5'-AATTCAAAAATTCTCCGAACGTGT CACGTTCTTTGAAACGTGACACGTTCCG AGAA-3'